Figure S1

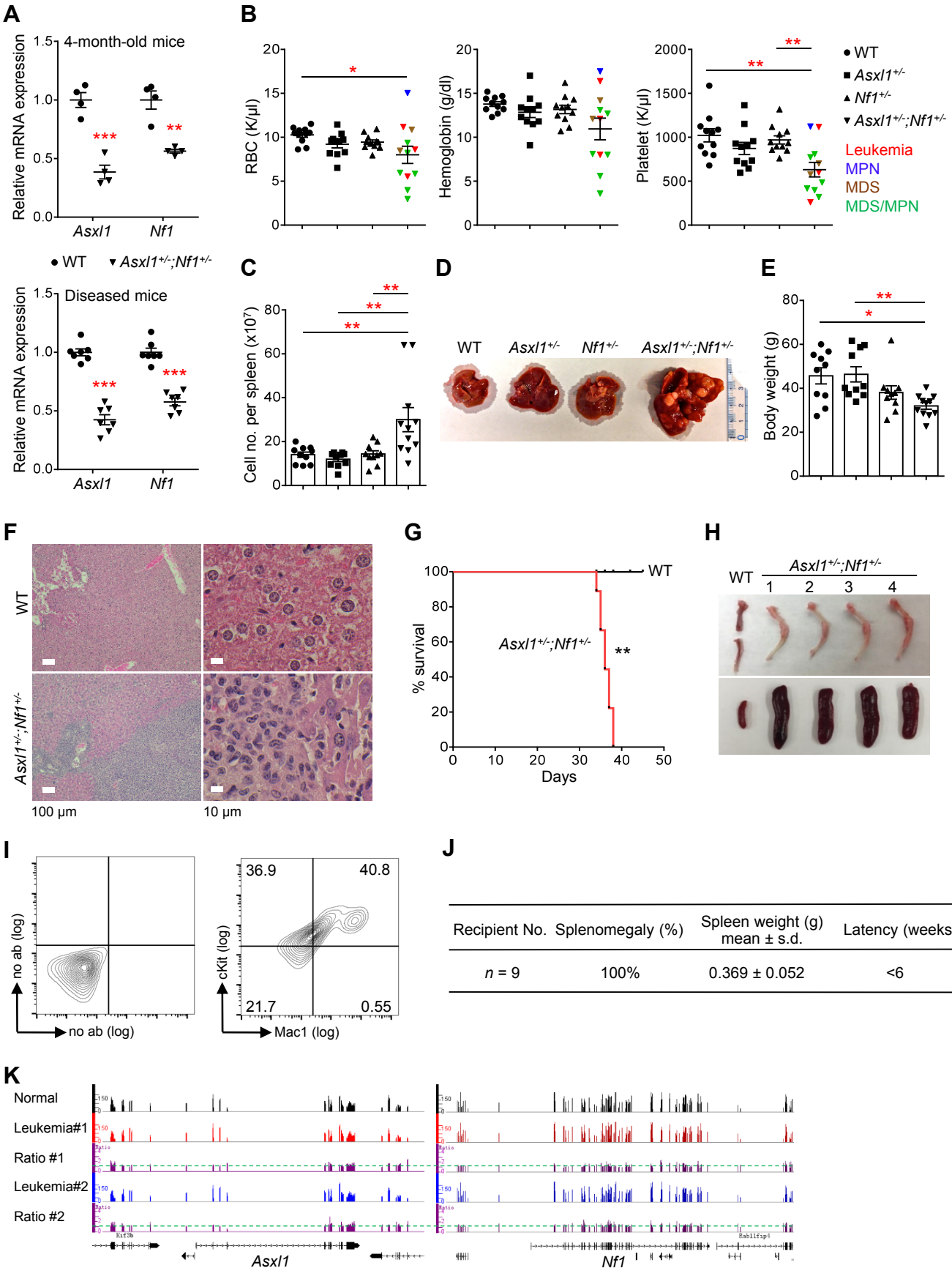

Recipient No.	Splenomegaly (%)	Spleen weight (g) mean ± s.d.	Latency (weeks)
n = 9	100%	0.369 ± 0.052	<6

Figure S1. Development of myeloid leukemia in *Asxl1*$^{+/-}$;*Nf1*$^{+/-}$ mice. (A) qPCR results showing the mRNA levels of *Asxl1* and *Nf1* in WT and *Asxl1*$^{+/-}$;*Nf1*$^{+/-}$ mice. Top, BM cKit^{+} cells from 4-month-old *Asxl1*$^{+/-}$;*Nf1*$^{+/-}$ mice (*n* = 4 per group); bottom, spleen cells from diseased *Asxl1*$^{+/-}$;*Nf1*$^{+/-}$ mice (*n* = 7 per group, two with myeloid leukemia and five with MDS/MPN in *Asxl1*$^{+/-}$;*Nf1*$^{+/-}$ mice). (B) Parameters of PB were summarized from WT, *Asxl1*$^{+/-}$, *Nf1*$^{+/-}$, and *Asxl1*$^{+/-}$;*Nf1*$^{+/-}$ mice at the time of sacrifice (*n* = 11 to 12 per group). (C) Spleen cellularity (*n* = 10 to 11 mice per group). (D) The gross morphologies of the liver from each genotype of mice. Tumors infiltrating liver in *Asxl1*$^{+/-}$;*Nf1*$^{+/-}$ mice. (E) Body weight of WT, *Asxl1*$^{+/-}$, *Nf1*$^{+/-}$ and *Asxl1*$^{+/-}$;*Nf1*$^{+/-}$ mice at the time of sacrifice (*n* = 10 to 11 per group). (F) Representative H&E stained sections from the liver of WT and *Asxl1*$^{+/-}$;*Nf1*$^{+/-}$ mice are shown. Scale bar: left, 100 μm; right, 10 μm. (G) Kaplan-Meier survival curve of secondary recipient mice transplanted with *Asxl1*$^{+/-}$;*Nf1*$^{+/-}$ spleen cells (WT, *n* = 5 and *Asxl1*$^{+/-}$;*Nf1*$^{+/-}$ *n* = 9). A log-rank test was used for survival statistics. (H) Representative photographs of bone and spleen from secondary recipient mice transplanted with *Asxl1*$^{+/-}$;*Nf1*$^{+/-}$ spleen cells at 6-week after transplantation. (I) Flow cytometric analysis of BM cells revealed that the recipients had the similar Mac1^{+}/cKit^{+} population with the primary mouse. (J) Enlargement of spleens from secondary recipient mice transplanted with *Asxl1*$^{+/-}$;*Nf1*$^{+/-}$ spleen cells at 6-week after transplantation. (K) *Asxl1* and *Nf1* gene coverages and read depth ratios obtained through whole exome sequencing of *Asxl1*$^{+/-}$;*Nf1*$^{+/-}$ leukemia cells (*n* = 2) and matched normal tissue. Data represent mean ± SEM. **P* < 0.05; ***P* < 0.01; ****P* < 0.001; unpaired Student's *t*-test (A) or one-way ANOVA with Tukey's multiple comparisons test (B-C, and E).

Figure S2

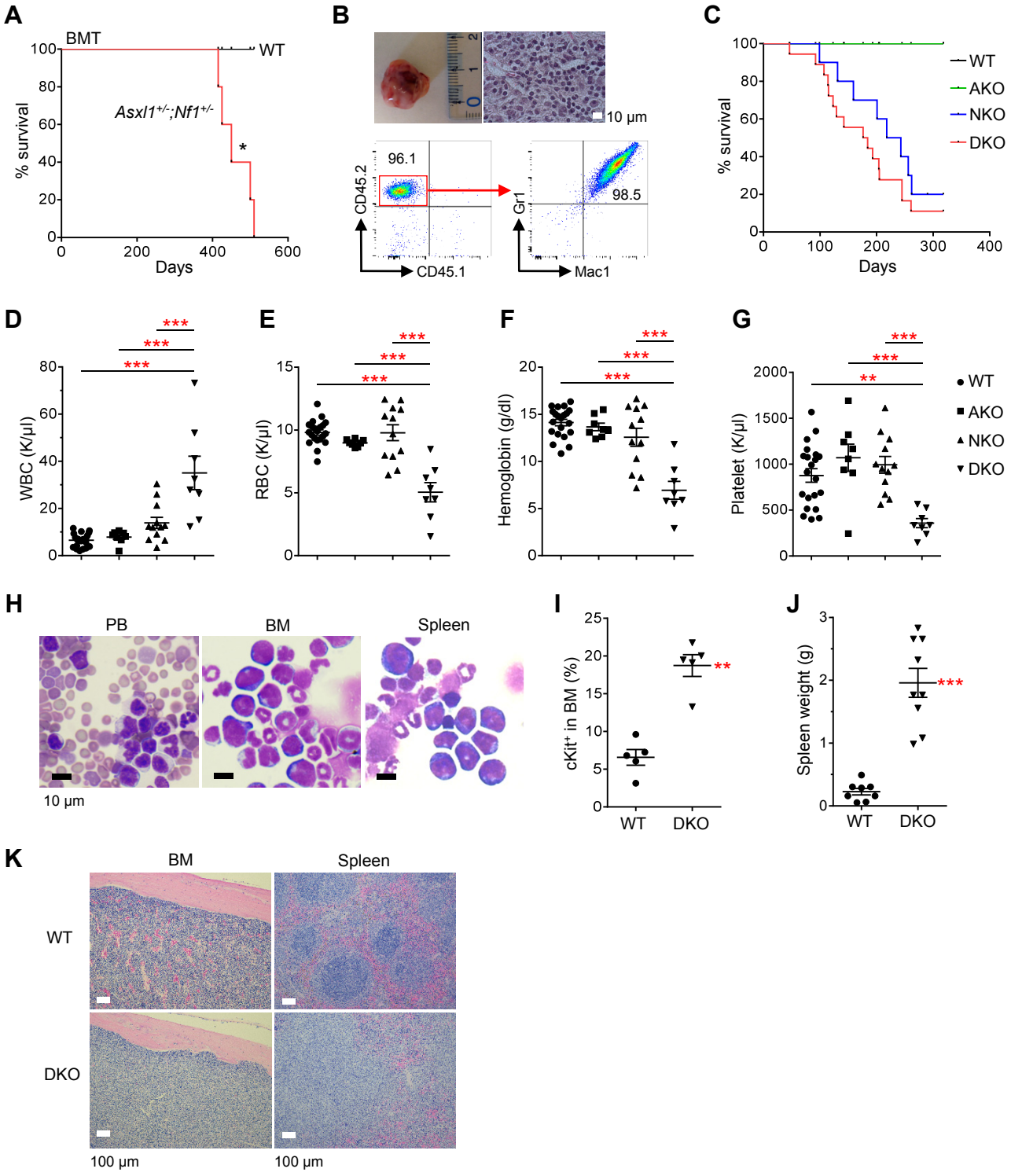
A
BMT
WT
Asxl1+/-;Nf1+/-
% survival
Days
B
10 μm
96.1
98.5
CD45.2
CD45.1
Gr1
Mac1
C
WT
AKO
NKO
DKO
% survival
Days
D
WBC (K/μl)
E
RBC (K/μl)
F
Hemoglobin (g/dl)
G
Platelet (K/μl)
WT
AKO
NKO
DKO
H
PB
BM
Spleen
10 μm
I
cKit+ in BM (%)
WT
DKO
J
Spleen weight (g)
WT
DKO
K
BM
Spleen
WT
DKO
100 μm
100 μm

Figure S2. Deletion of *Asxl1* and *Nf1* accelerates the development of myeloid leukemia in vivo. (A) Kaplan-Meier curve representing percent survival of recipient mice transplanted with BM cells from WT and young *Asxl1*$^{+/-}$;*Nf1*$^{+/-}$ mice (*n* = 5 per group). No lethality was observed for recipients of WT BM cells. A log-rank test was used for survival statistics. (B) The appearance of one *Asxl1*$^{+/-}$;*Nf1*$^{+/-}$ transplanted mouse (*n* = 5) with a large mass in the stomach (left panel). Representative microphotograph of H&E stained section of the mass (right panel). Below is the flow cytometric analysis of the cells within the large mass. (C) Kaplan-Meier survival curve showing the percent survival of WT (*n* = 10), *Asxl1*$^{\Delta/\Delta}$ (AKO, *n* = 5), *Nf1*$^{\Delta/\Delta}$ (NKO, *n* = 10) and DKO (*n* = 18) mice over time. (D-G) Peripheral WBC count (D), RBC count (E), Hemoglobin (F), and Platelets (G) for each genotype of mice (*n* = 8 to 21 per group) at time of sacrifice (3-6 months after pIpC injection). (H) May-Grunwald-Giemsa-stained blood smear and cytospin preparations of BM and spleen cells from WT and DKO mice. Scale bar: 10 μm. (I) Flow cytometric analysis of the BM cells revealed a significantly increased cKit^{+} population in DKO mice (*n* = 5 per group). (J) Spleen weight from WT and DKO mice is shown (*n* = 8 to 9 per group). (K) Representative H&E stained sections from femur and spleen from WT and DKO mice are shown. Scale bar: 100 μm. Data represent mean ± SEM. **P* < 0.05; ***P* < 0.01; ****P* < 0.001; one-way ANOVA with Tukey's multiple comparisons test (D-G) or unpaired Student's *t*-test (I and J).

Figure S3

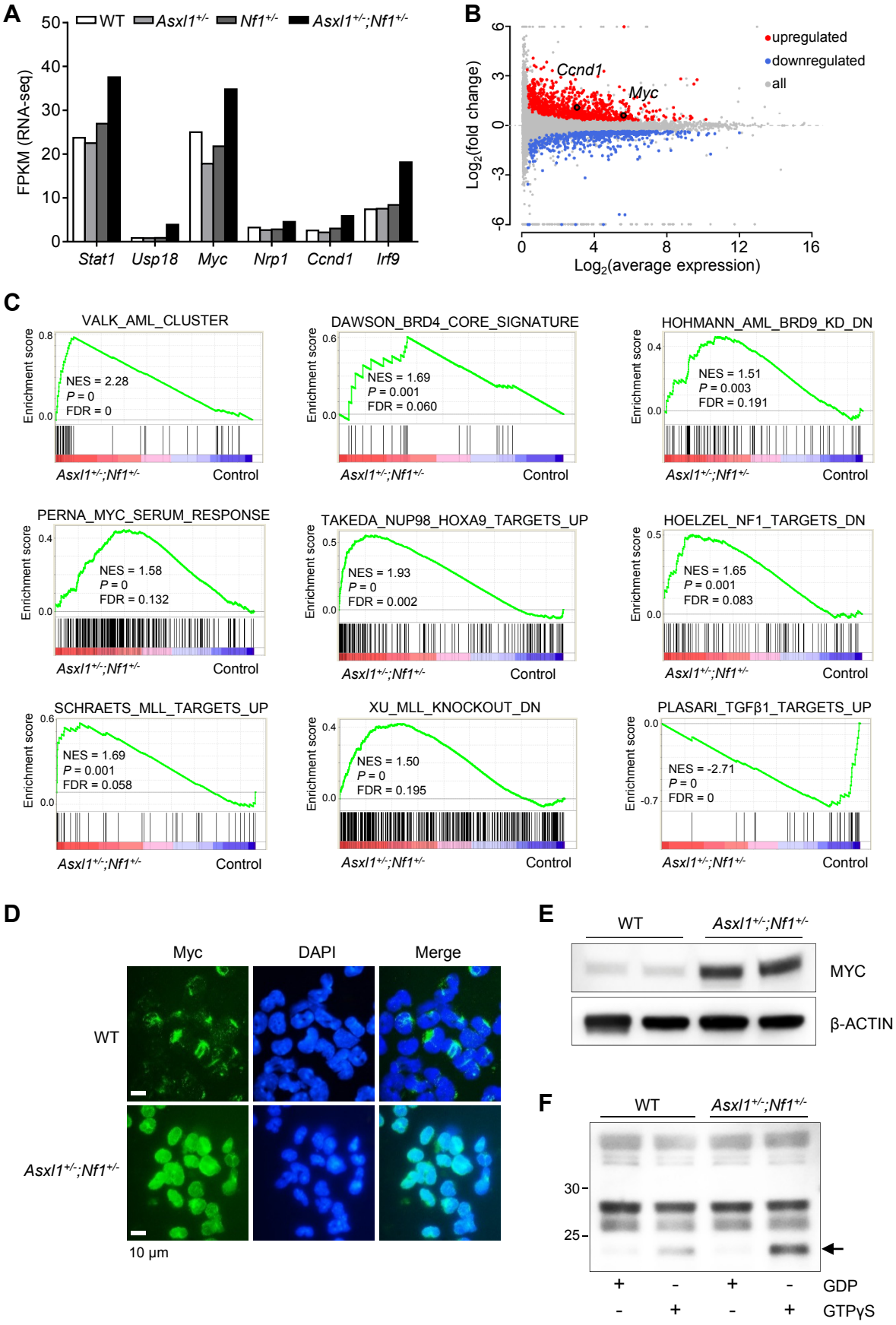
A
WT
Asxl1+/-
Nf1+/-
Asxl1+/-;Nf1+/-
FPKM (RNA-seq)
Stat1
Usp18
Myc
Nrp1
Ccnd1
Irf9
B
upregulated
downregulated
all
Ccnd1
Myc
Log2(fold change)
Log2(average expression)
C
VALK_AML_CLUSTER
NES = 2.28
P = 0
FDR = 0
DAWSON_BRD4_CORE_SIGNATURE
NES = 1.69
P = 0.001
FDR = 0.060
HOHMANN_AML_BRD9_KD_DN
NES = 1.51
P = 0.003
FDR = 0.191
PERNA_MYC_SERUM_RESPONSE
NES = 1.58
P = 0
FDR = 0.132
TAKEDA_NUP98_HOXA9_TARGETS_UP
NES = 1.93
P = 0
FDR = 0.002
HOELZEL_NF1_TARGETS_DN
NES = 1.65
P = 0.001
FDR = 0.083
SCHRAETS_MLL_TARGETS_UP
NES = 1.69
P = 0.001
FDR = 0.058
XU_MLL_KNOCKOUT_DN
NES = 1.50
P = 0
FDR = 0.195
PLASARI_TGFβ1_TARGETS_UP
NES = -2.71
P = 0
FDR = 0
Enrichment score
Asxl1+/-;Nf1+/-
Control
D
Myc
DAPI
Merge
WT
Asxl1+/-;Nf1+/-
10 μm
E
WT
Asxl1+/-;Nf1+/-
MYC
β-ACTIN
F
WT
Asxl1+/-;Nf1+/-
30
25
GDP
GTPγS

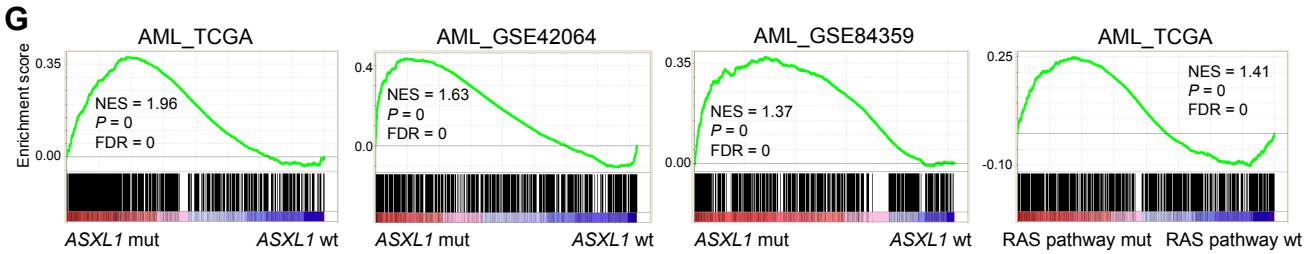

H

AML_TCGA (*ASXL1* mut vs *ASXL1* wt)	AML_GSE42064 (*ASXL1* mut vs *ASXL1* wt)	AML_GSE84359 (*ASXL1* mut vs *ASXL1* wt)	AML_TCGA (RAS pathway mut vs RAS pathway wt)
mouse 793 / 38 / human 453 *P* = 1.2e-4	mouse 824 / 7 / human 57 *P* = 7.2e-3	mouse 817 / 14 / human 129 *P* = 2.3e-4	mouse 810 / 21 / human 305 *P* = 0.026
USP18, NRP1, IRF7, IRF8, CXCL12, TNC, UGCG, MX1, IFI27, LGMN, OAF, CARD11, LPL, SIGLEC1, ZBP1, AMIGO2, ISG20, GSTM5, ISG15, COL1A2, FSTL1, CXCR3, SLC25A21, TGFBI, ACHE, EPSTI1, FABP4, IGFBP5, ABCG2, GJA1, PKDCC, IL10RA, NINL, FCRL5, IFIT1, SEMA6D, CD22, OAS2	*CXCL12, GJA1, CDC42BPA, FAM213A, MMP8, PLSCR4, SPARC*	*LGALS3BP, UGCG, ACSL6, ABCB6, IFI27, EPB42, ABCG2, RHAG, PLS1, HEMGN, GYPA, GCLM, TMCC2, TMEM51*	*USP18, OAF, SAMD14, MYL9, MX1, OAS3, ISG15, SIGLEC1, NRIP1, GP6, CXCR3, IFIT1, PPBP, IFI27, EPSTI1, CD22, COL5A1, NCR1, ALDH1A1, WBSCR27, CLEC9A*

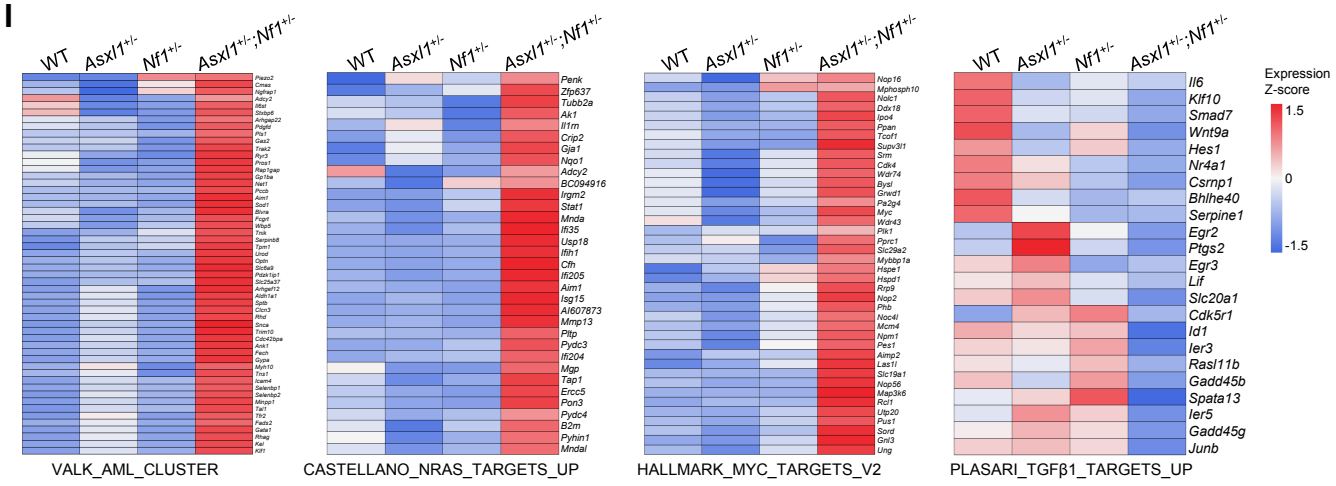

J

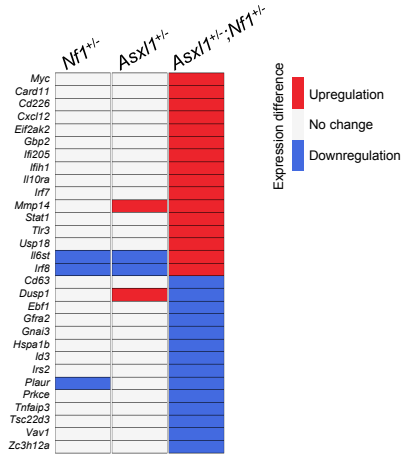

Figure S3. Cooperative effect of *Asxl1* and *Nf1* loss on the induction of a MYC-driven transcription signature. (A) Fragments per kilobase of transcript per million (FPKM) values of DEGs in RNA-seq are shown. Data represent the mean of two biological replicates. (B) MA plot showing the dysregulated genes in *Asxl1*$^{+/-}$;*Nf1*$^{+/-}$ cKit^{+} cells compared with WT and single mutant cells. *Myc* and *Ccnd1* are highlighted in black. (C) GSEA showing expression differences of representative transcription signatures associated with AML, MYC, and MYC upregulators BRD4/9, NUP98-HOXA9, NF1, MLL, and TGFβ target genes in *Asxl1*$^{+/-}$;*Nf1*$^{+/-}$ cKit^{+} cells compared with control cells. (D) Immunofluorescence assay shows the MYC protein accumulation (Green) in *Asxl1*$^{+/-}$;*Nf1*$^{+/-}$ BMMNCs compared with WT cells. Nuclei were visualized with DAPI (Blue). Scale bars: 10 μm. (E) Western blot showing the MYC protein levels in *Asxl1*$^{+/-}$;*Nf1*$^{+/-}$ and WT BMMNCs. (F) Activated RAS protein (RAS-GTP) was quantified in *Asxl1*$^{+/-}$;*Nf1*$^{+/-}$ BMMNCs via immunoprecipitation with the RAS-binding domain of RAF (RAF-1 RBD) followed by immunoblot using anti-RAS antibody. (G) GSEA showing that genes upregulated in *Asxl1*$^{+/-}$;*Nf1*$^{+/-}$ cKit^{+} cells are enriched in AML patients with *ASXL1* or RAS pathway gene mutations compared with patients without those mutations. (H) Overlap of genes aberrantly overexpressed in *ASXL1* or RAS-mutated AML patients and in *Asxl1*$^{+/-}$;*Nf1*$^{+/-}$ cKit^{+} cells. *P* values were calculated by two-tailed Fisher's exact test with GeneOverlap. (I) Leading edge genes in representative signatures that were obtained from GSEA analyses display increased or decreased expression specific to *Asxl1*$^{+/-}$;*Nf1*$^{+/-}$ cKit^{+} cells. (J) Heatmap displaying expression difference of master regulators predicted with DEGs of *Asxl1*$^{+/-}$;*Nf1*$^{+/-}$ in single mutant cells compared with WT.

Figure S4

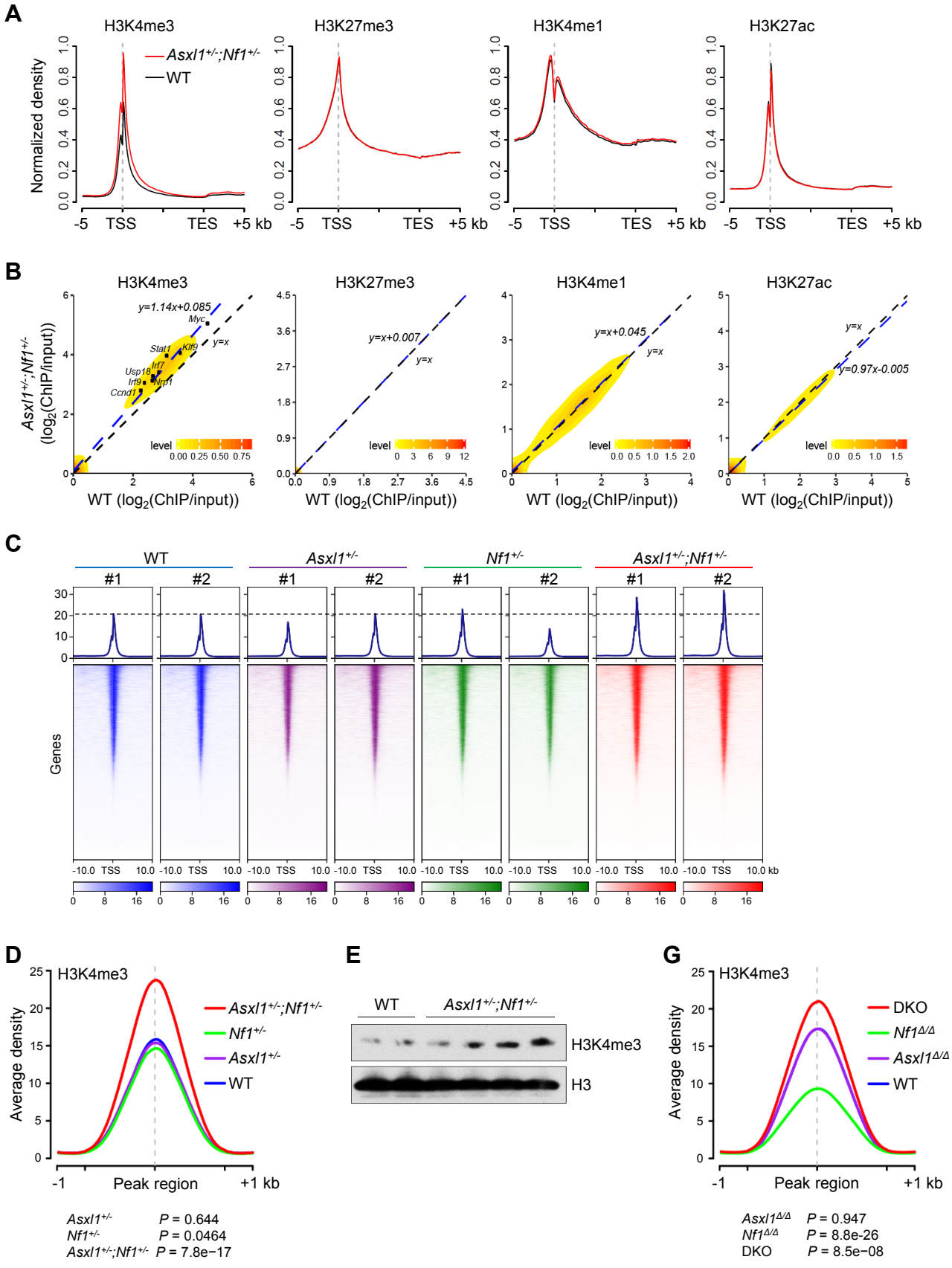
A
H3K4me3
H3K27me3
H3K4me1
H3K27ac
Asxl1+/-;Nf1+/-
WT
Normalized density
-5 TSS TES +5 kb
B
H3K4me3
H3K27me3
H3K4me1
H3K27ac
y=1.14x+0.085
y=x
y=x+0.007
y=x+0.045
y=0.97x-0.005
Myc
Stat1
Klf9
Irf7
Usp18
Irf9
Ncf1
Ccnd1
level
Asxl1+/-;Nf1+/- (log2(ChIP/input))
WT (log2(ChIP/input))
C
WT
Asxl1+/-
Nf1+/-
Asxl1+/-;Nf1+/-
#1
#2
Genes
-10.0 TSS 10.0
10.0 kb
D
H3K4me3
Asxl1+/-;Nf1+/-
Nf1+/-
Asxl1+/-
WT
Average density
-1 Peak region +1 kb
Asxl1+/- P = 0.644
Nf1+/- P = 0.0464
Asxl1+/-;Nf1+/- P = 7.8e−17
E
WT
Asxl1+/-;Nf1+/-
H3K4me3
H3
G
H3K4me3
DKO
Nf1Δ/Δ
Asxl1Δ/Δ
WT
Average density
-1 Peak region +1 kb
Asxl1Δ/Δ P = 0.947
Nf1Δ/Δ P = 8.8e-26
DKO P = 8.5e−08

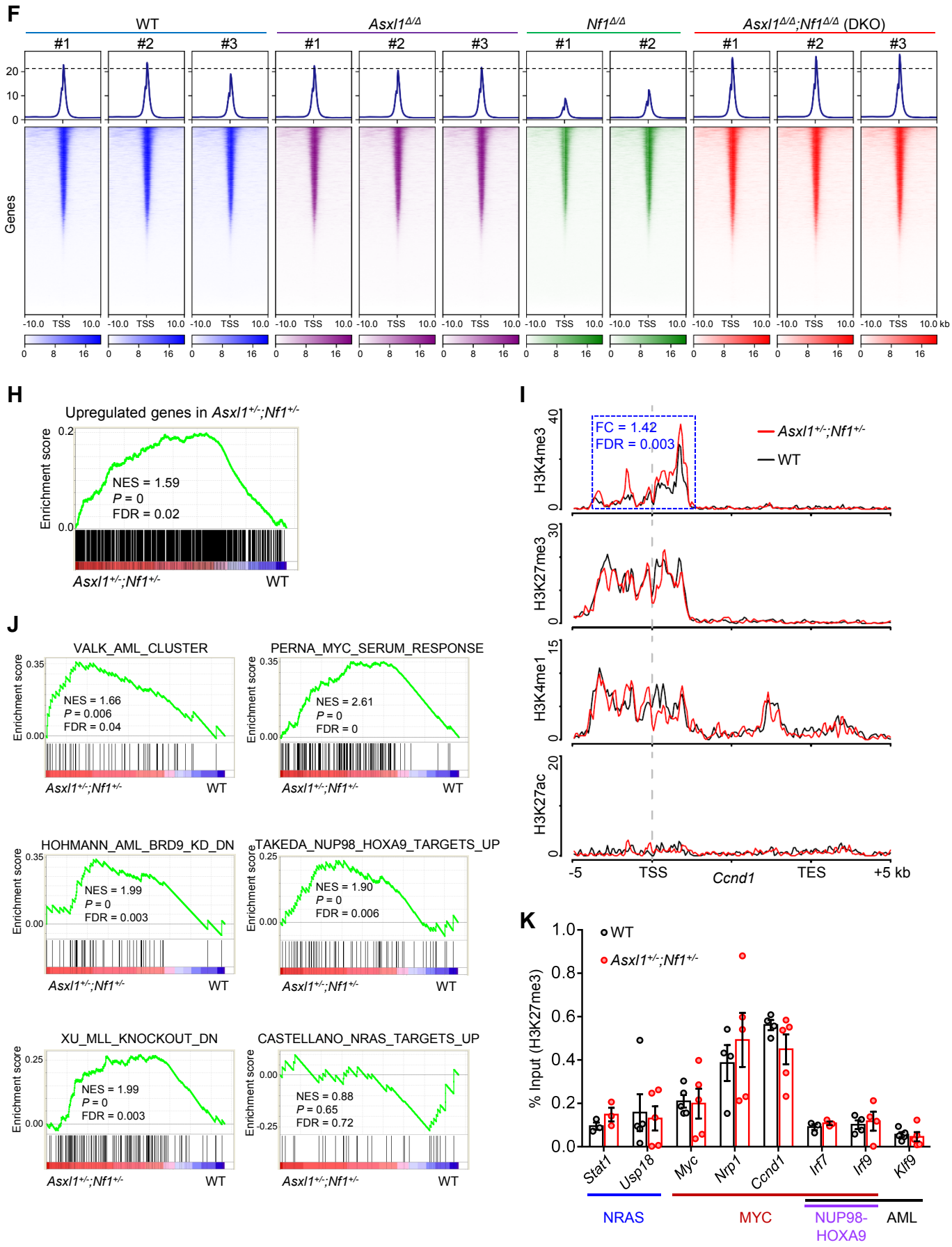
F
WT
Asxl1Δ/Δ
Nf1Δ/Δ
Asxl1Δ/Δ;Nf1Δ/Δ (DKO)
#1
#2
#3
Genes
-10.0 TSS 10.0
10.0 kb
H
Upregulated genes in Asxl1+/-;Nf1+/-
Enrichment score
NES = 1.59
P = 0
FDR = 0.02
Asxl1+/-;Nf1+/-
WT
I
FC = 1.42
FDR = 0.003
Asxl1+/-;Nf1+/-
WT
H3K4me3
H3K27me3
H3K4me1
H3K27ac
-5
TSS
Ccnd1
TES
+5 kb
J
VALK_AML_CLUSTER
NES = 1.66
P = 0.006
FDR = 0.04
PERNA_MYC_SERUM_RESPONSE
NES = 2.61
P = 0
FDR = 0
HOHMANN_AML_BRD9_KD_DN
NES = 1.99
P = 0
FDR = 0.003
TAKEDA_NUP98_HOXA9_TARGETS_UP
NES = 1.90
P = 0
FDR = 0.006
XU_MLL_KNOCKOUT_DN
NES = 1.99
P = 0
FDR = 0.003
CASTELLANO_NRAS_TARGETS_UP
NES = 0.88
P = 0.65
FDR = 0.72
K
WT
Asxl1+/-;Nf1+/-
% Input (H3K27me3)
Stat1
Usp18
Myc
Nrp1
Ccnd1
Irf7
Irf9
Klf9
NRAS
MYC
NUP98-HOXA9
AML

Figure S4. Increased H3K4me3 enrichment contributes to aberrant activation of key signatures in *Asxl1*$^{+/-}$;*Nf1*$^{+/-}$ cKit^{+} cells. (A) Global levels of histone modifications at genes and flanking 5 kb regions. For ease of comparison, coverages normalized by sequencing depth were scaled to 100% and averaged in two biological replicates. (B) 2D Kernel Density plots showing relative enrichment intensity of histone modifications at each gene locus ranging from upstream 5 kb to downstream 5 kb of transcription start site (TSS ± 5kb). The x-axis and y-axis show $\log_2$ transformed enrichment fold (ChIP/input) averaged in two biological replicates. Genes shown in Figure 3D are highlighted in black points. Dashed blue line: linear fit. Dashed black line: y = x. (C and F) Density plot displaying H3K4me3 occupancies centered on TSSs in each genotype of mice, respectively. Each row represents a single gene. (D and G) Global levels of H3K4me3 at enriched and flanking 1 kb regions. For ease of comparison, normalized coverages by sequencing depth were averaged in 2 or 3 biological replicates. Statistical analysis was performed using unpaired Student's *t*-test to determine H3K4me3 difference between WT and other genotypes. (E) Western blot analysis showing the global H3K4me3 levels in *Asxl1*$^{+/-}$;*Nf1*$^{+/-}$ and WT cKit^{+} cells. H3 was used as a loading control. (H) GSEA plot showing an increase in H3K4me3 occupancies at TSS ± 5 kb for all 831 upregulated genes in *Asxl1*$^{+/-}$;*Nf1*$^{+/-}$ cKit^{+} cells. NES, *P,* and FDR values are shown. (I) Normalized ChIP-binding signals are displayed for four histone modifications on the *Ccnd1* gene. The y-axis represents the normalized read density that was averaged in two biological replicates. The identified DER and its statistical difference between *Asxl1*$^{+/-}$;*Nf1*$^{+/-}$ versus WT cells are indicated in a blue box. (J) GSEA plots showing enrichment of the indicated signatures consisting of activated genes marked by promoter H3K4me3 occupancies in *Asxl1*$^{+/-}$;*Nf1*$^{+/-}$ versus WT cells. NES, *P*, and FDR values are shown. (K) ChIP-qPCR showing the enrichment of H3K27me3 on key gene promoters (*n* = 3 to 5 mice per group). Data represent mean ± SEM.

Figure S5

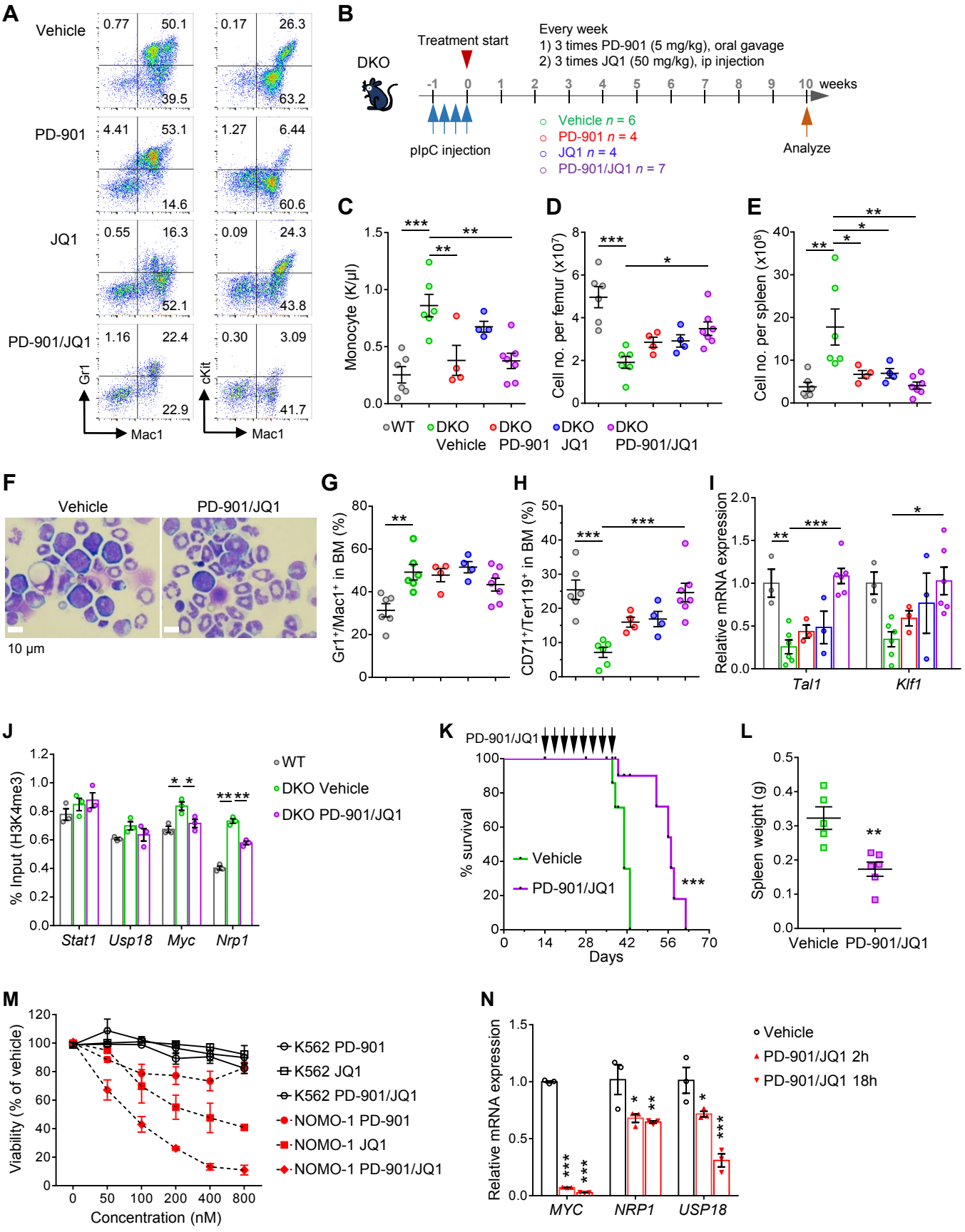
A
Vehicle
PD-901
JQ1
PD-901/JQ1
Gr1
Mac1
cKit
Mac1
B
DKO
Treatment start
Every week
1) 3 times PD-901 (5 mg/kg), oral gavage
2) 3 times JQ1 (50 mg/kg), ip injection
weeks
pIpC injection
Vehicle n = 6
PD-901 n = 4
JQ1 n = 4
PD-901/JQ1 n = 7
Analyze
C
Monocyte (K/μl)
D
Cell no. per femur (x10⁷)
E
Cell no. per spleen (x10⁸)
WT
DKO Vehicle
DKO PD-901
DKO JQ1
DKO PD-901/JQ1
F
Vehicle
PD-901/JQ1
10 μm
G
Gr1⁺/Mac1⁺ in BM (%)
H
CD71⁺/Ter119⁺ in BM (%)
I
Relative mRNA expression
Tal1
Klf1
J
% Input (H3K4me3)
Stat1
Usp18
Myc
Nrp1
WT
DKO Vehicle
DKO PD-901/JQ1
K
PD-901/JQ1
% survival
Vehicle
PD-901/JQ1
Days
L
Spleen weight (g)
Vehicle
PD-901/JQ1
M
Viability (% of vehicle)
Concentration (nM)
K562 PD-901
K562 JQ1
K562 PD-901/JQ1
NOMO-1 PD-901
NOMO-1 JQ1
NOMO-1 PD-901/JQ1
N
Relative mRNA expression
MYC
NRP1
USP18
Vehicle
PD-901/JQ1 2h
PD-901/JQ1 18h

Figure S5. Inhibition of the MAPK pathway and MYC using PD-901 and JQ1 eradicate leukemogenesis in vivo. (A) Liquid cultures of DKO BM cells with PD-901, JQ1, or PD-901/JQ1 for 3 days. Flow cytometric analyses showing the percentage of $Gr1^+/Mac1^+$ and $cKit^+/Mac1^+$ cells (*n* = 3 mice per group from 2 independent experiments). (B) Schema of PD-901 and JQ1 treatment in vivo (*n* = 4 to 7 mice per group). (C) Peripheral monocyte count. (D) Bone marrow cellularity (femur) for each group of mice. (E) Spleen cell number. (F and G) Mature myeloid cells were observed in the PD-901 and/or JQ1 treated groups compared with the vehicle controls. (H and I) Erythroid differentiation was restored in the PD-901/JQ1 treated group. The frequency of $CD71^+/Ter119^+$ cells were significantly increased (H) and the expression level of erythroid transcription factors *Tal1* and *Klf1* were significantly increased (I) in the PD-901/JQ1 treatment group (*n* = 3 to 6 mice per group). (J) ChIP-qPCR shows the enrichment of H3K4me3 in the key DEGs (*n* = 3 mice per group). (K) Survival curve of the $Asxl1^{+/-};Nf1^{+/-}$ recipient mice treated with vehicle or combination of PD-901 and JQ1. The treatment began 14 days after $Asxl1^{+/-};Nf1^{+/-}$ leukemic cell transplant (*n* = 5 to 6 mice per group). A log-rank test was used for survival statistics. (L) Spleen weight was measured after 3 weeks of the treatment. (M) Dose-response of human AML cell lines to PD-901 and JQ1. Cells were treated with vehicle or indicated inhibitors for 3 days and viable cells were counted by flow cytometry. Cell numbers were normalized to vehicle treated controls. The graph shows an average of three independent experiments. (N) qPCR showing the expression levels of *MYC*, *NRP1* and *USP18* were significantly decreased after the treatment of PD-901/JQ1. Data represent mean ± SEM. $*P < 0.05$; $**P < 0.01$; $***P < 0.001$; one-way ANOVA with Tukey's multiple comparisons test (C-E and G-J) or unpaired Student's *t*-test (L and N).

Table S1. Diagnosis of MDS, MPN and MDS/MPN developed in 12 *Asxl1*$^{+/-}$;*Nf1*$^{+/-}$ mice.

Survival (Months)	Blood counts	Blasts (%)	Dysplastic Neutrophil	Necropsy and other findings	Diagnosis and subclassification
15-16 (*n* = 2)	WBC ↓ NE →↑ MO ↓ RBC → PLT ↓	< 20%	Yes	Splenomegaly	MDS
13 (*n* = 1)	WBC ↑ NE ↑ MO → RBC ↑ PLT →	< 20%	No	Splenomegaly	MPN
8-16 (*n* = 6)	WBC →↓ NE →↑ MO → RBC →↓ PLT →↓	< 20%	Yes	splenomegaly	MDS/MPN

Table S2. Diagnosis of myeloid leukemia developed in 12 *Asxl1*$^{+/-}$;*Nf1*$^{+/-}$ mice.

Survival (days)	Blood counts	Blasts (%)	Necropsy and other findings	Diagnosis and subclassification
395	WBC ↑ NE ↑ MO → RBC → PLT →	> 20%	Splenomegaly	Myeloid leukemia
425	WBC ↑ NE ↑ MO → RBC → PLT →	> 20%	Splenomegaly	Myeloid leukemia (tumor in stomach)
510	WBC ↑ NE ↑ MO → RBC ↓ PLT ↓	> 20%	Hepato-splenomegaly	Myeloid leukemia (tumor in liver)

Table S3. Somatic single nucleotide variants and indels identified in 2 *Asxl1*$^{+/-}$*;Nf1*$^{+/-}$ leukemias through whole exome sequencing. (Excel file)

Table S4. Differentially expressed genes from RNA-seq. (Excel file)

Table S5. Gene panel for targeted sequencing used in this study.

ABL1	*CREBBP*	*FGFR3*	*JAK3*	*NOTCH2*	*SETBP1*	*TET2*
ASXL1	*CSF3R*	*FLT3*	*KIT*	*NPM1*	*SF1*	*TNFAIP3*
ATM	*CUX1*	*GATA1*	*KMT2D*	*NRAS*	*SF3A1*	*TP53*
BCOR	*DNMT3A*	*GATA2*	*KRAS*	*PAX5*	*SF3B1*	*U2AF1*
BCORL1	*DNMT3B*	*GATA3*	*MLL*	*PHF6*	*SH2B3*	*U2AF2*
BRAF	*EED*	*IDH1*	*MPL*	*PRPF40B*	*SMC1A*	*WT1*
CALR	*EP300*	*IDH2*	*MYC*	*PTEN*	*SMC3*	*ZRSR2*
CBL	*ETV6*	*IKZF1*	*MYD88*	*PTPN11*	*SRSF2*	
CCND3	*EZH2*	*JAK1*	*NF1*	*RB1*	*SUZ12*	
CEBPA	*FBXW7*	*JAK2*	*NOTCH1*	*RUNX1*	*TAL1*	

Table S6. RAS pathway gene mutations identified in 138 cases with myeloid malignancies. (Excel file)

Table S7. Comparison of clinical characteristics by RAS pathway gene mutation status in myeloid malignancies.

Characteristic	RAS pathway gene mutated (*n* = 35) no. (%)	RAS pathway gene wt (*n* = 103) no. (%)	*P*
Age, years			0.432
Median	43	47	
Range	22-73	25-68	
Sex			0.427
Male	20 (57%)	55 (53%)	
Female	15 (43%)	48 (47%)	
Diagnosis			0.033
AML	17 (48.6)	30 (29.1)	0.041
MDS	7 (20)	45 (43.7)	0.015
MPN	3 (8.6)	26 (25.2)	0.027
MDS/MPN	8 (22.9)	2 (1.9)	<0.001
Bone marrow blasts (%)			0.027
Median	15.5	2	
Range	0-93.5	0-92.5	
WBC count (x10^9/L)			0.084
Median	45.46	4.68	
Range	1.59-182.83	0.13-258	
Hemoglobin (g/L)			0.020
Median	81	96	
Range	33-152	18-195	
Platelet count (x10^9/L)			0.001
Median	51	75	
Range	8-695	3-3149	

Table S8. Revised International Prognostic Scoring System risk category for MDS patients with *ASXL1* and/or RAS pathway gene mutations.

MDS patients	Very Low	Low	Intermediate	High	Very High
RAS gene mutated	14.3 (1/7)	14.3 (1/7)	14.3 (1/7)	14.3 (1/7)	28.6 (2/7)
RAS gene WT	0.0 (0/45)	44.3 (20/45)	28.9 (13/45)	20.0 (9/45)	6.7 (3/45)

Table S9. Flow antibodies used in this study.

Antibody name	Clone	Color	Catalog	Company
Rat anti-Mouse CD34	RAM34	FITC	553733	BD Pharmingen
Rat anti-Mouse Ly-6A/E (Sca1)	D7	PE-Cy7	558162	BD Pharmingen
Rat anti-Mouse CD117	2B8	PE	553355	BD Pharmingen
Rat anti-Mouse CD117	2B8	APC	553356	BD Pharmingen
Rat anti-Mouse CD117	2B8	PerCP-Cy5.5	560557	BD Pharmingen
Rat anti-Mouse CD16/CD32	2.4G2	APC-Cy7	560541	BD Pharmingen
Rat anti-mouse CD135	A2F10.1	BV421	562898	BD Horizon
Mouse Lineage Antibody Cocktail		APC	558074	BD Pharmingen
Rat anti-Mouse CD71	C2	FITC	553266	BD Pharmingen
Rat anti-Mouse TER-119	TER-119	APC	557909	BD Pharmingen
Rat anti-Mouse Ly-6G and Ly-6C	RB6-8c5	PerCP-Cy5.5	552093	BD Pharmingen
Rat anti-Mouse CD11b	M1/70	PE	553311	BD Pharmingen
Mouse anti-Mouse CD45.2	104	PerCP-Cy5.5	552950	BD Pharmingen
Mouse anti-Mouse CD45.1	A20	FITC	553775	BD Pharmingen
7-AAD		PerCP-Cy5.5	559925	BD Pharmingen

Table S10. Primers used for in this study.

Gene Name	Forward	Reverse
qPCR-mouse		
Asxl1	TCACACCGAAAAGCCACAG	GGGCATATCTGGTAAGTGGG
Nf1	CTTGAGGAGAACCAGAGGAAC	CAGTAGGGAGTGGCAAGTTG
Myc	AGAGCTCCTCGAGCTGTTTG	TGAAGTTCACGTTGAGGGG
Nrp1	CCGGAACCCTACCAGAGAA	CCCCATCAATTACTTCCACG
Stat1	TCCCGTACAGATGTCCATGAT	CTGAATATTTCCCTCCTGGG
Usp18	CTGCAGAAATACAACGTGCC	GTGTCCGTGATCTGGTCCTT
Ccnd1	TCCTCTCCAAAATGCCAGAG	GGGTGGGTTGGAAATGAAC
Irf7	TGATCCGCATAAGGTGTACG	AGCATTGCTGAGGCTCACTT
Irf9	TGAGCTAGAGGAGGGAGCTG	ACTCGGCCACCATAGATGAA
Klf9	CCTCCCATCTTAAAGCCCAT	AGCGCGAGAACTTTTTAAGG
Actb	GGCTGTATTCCCCTCCATCG	CCAGTTGGTAACAATGCCATGT
Tal1	CCCCATGTTCACCAACAAC	CCGCACTACTTTGGTGTGAG
Klf1	CTTTGGCACCTAAGAGGCAG	CAGGAGCAGGCATAAGGC
qPCR-human		
MYC	TTTCGGGTAGTGGAAAACCA	CACCGAGTCGTAGTCGAGGT
NRP1	GAAAAATGCGAATGGCTGAT	TTGCAGTCTCTGTCCTCCAA
USP18	AGTCCCGACGTGGAACTCAG	CAGCACGACTTCACTTCCAG
ACTB	GCACAGAGCCTCGCCTT	CCTTGCACATGCCGGAG
ChIP-qPCR		
Myc	GATCTGAGTCGGGGTAGAGC	AACCCCGCTTCAAAATGCAT
Nrp1	TCTCGCGAATTCAGGCATTG	CCGAAACGCTCTTAAGTCCG
Stat1	GCCGTTCTCACTTCTAGGGT	AAGGCGAGCAAAGGTTAAGC
Usp18	TCGCAGAGCTGTACCTTCAT	CTCTGACCAGTCCCACCATT
Ccnd1	GCATGTTCGTGGCCTCTAAG	AAAGAGGGATTGTCGGTGGT
Irf7	AGGGTCGGGTGTAGTTTGAG	AAACAGTCTAAACAGCGCCC
Irf9	CTGCCCATTTCTTCAGCTCC	AAGGCATCTATCTCCCCAGC
Klf9	GAGTTGAATCACCCTCCCCA	CGGCATTCTCCAGCTCAGTA